PERGAMON

International Journal of Heat and Mass Transfer 43 (2000) 1035–1050

International Journal of HEAT and MASS TRANSFER

www.elsevier.com/locate/ijhmt

The heating, by viscous dissipation, of liquids flowing across an enclosed rotating disc

C.M. Ellwood [a,*], W.J. Korchinsky [b]

[a] EA Technology Ltd, Capenhurst, Chester CH1 6ES, UK
[b] Department of Chemical Engineering, UMIST, Manchester M60 1QD, UK

Received 27 July 1998; received in revised form 28 April 1999

Abstract

An experimental study confirmed that viscous dissipation energy generated by closely spaced discs, one of which is rotated at high speed, could be used to heat viscous fluids. The rate of viscous dissipation energy generated can be accurately predicted using simple theoretical methods. © 2000 Published by Elsevier Science Ltd. All rights reserved.

1. Introduction

Viscous dissipation in most heat transfer applications is of secondary importance. Velocity gradients within a viscous fluid must be high to generate significant energy by this mechanism. However, there are applications where significant influences of viscous dissipation occur. Dynamometers, first described by Froude in 1877 [1], utilise the principle in power measurement. In hydrokinetic brakes, mechanical energy is dissipated through viscous dissipation means.

Soo in 1958 [2] analysed laminar flow across an enclosed rotating disc. He derived expressions for the velocity components in the radial, tangential and axial directions, and for the radial variation in pressure. More on this later. The energy equation for laminar flow in this situation has been given by Dorfman [3], with the viscous heat generation term discussed by Owen and Rogers [4]. A simple Couette flow model described by Eckert and Drake [5] may also be used to predict heat generated by viscous dissipation.

Patents have been granted [6,7] which suggest the use of viscous dissipation for heating viscous fluids, but no practical application is known. The objectives of this work were to design and operate a machine whose primary purpose would be for heating viscous fluids by viscous dissipation, and to apply the theory to the prediction of the energy generated.

2. Experimental arrangements

2.1. Preliminary study — prototype machine

A preliminary study by Ellwood [8], to demonstrate experimentally that the concept could be applied, was carried out on a prototype, illustrated in Fig. 1.

The basis for the prototype viscous heating machine was a standard Worthington–Simpson centrifugal motor/pump unit, with a pumping capacity of 50 m^3 h^{-1} at 2900 rpm. The pump unit was modified to enhance viscous shear at the expense of pumping capacity by replacing the standard impeller with a plain disc (nominal dimensions of 130 mm diameter by 33 mm long). When installed, this disc was partially shrouded by a specially machined stator, fitted to the

* Corresponding author.

0017-9310/00/$ - see front matter
PII: S0017-9310(99)00183-0

Nomenclature

a, b	effective inner, outer, radius of disc respectively (m)
c_p	specific heat capacity at constant pressure (J kg^{-1} K^{-1})
f	general variable
g	acceleration due to gravity (m s^{-2})
G	gap ratio, Eq. (1)
H	enthalpy per unit mass (J kg^{-1})
l	width of disc, length of disc cylindrical gap (m)
m, m_f, m_r	mass flows, total, across front face of disc and across rear face of disc (kg s^{-1})
p	pressure (Pa)
p_a, p_b	pressures at inner and outer radius of gap, respectively (Pa)
r	radial co-ordinate (m)
Re_ϕ	rotational Reynolds number, Eq. (2)
Re_z	axial Reynolds number, defined by $\omega z_0^2/\nu$
Q	energy absorbed as heat from surroundings per unit mass (J kg^{-1})
t	times
T	temperature variable (K)
T_1–T_6	temperatures from machine inlet to machine outlet — Figs. 4 and 9 (K)
U	internal energy per unit mass (J kg^{-1})
u, v, w	velocity in radial, tangential and axial directions respectively (m s^{-1})
W_s	net work done by the liquid on the surroundings per unit mass (J kg^{-1})
V	mean velocity (m s^{-1})
X_c, X_f	viscous heat generation, cylindrical gap, across either face of disc (W)
z	axial co-ordinate (m)
z_0, y_0	axial and radial disc/casing gap, respectively (m)
Z	vertical distance above datum level (m)

Greek symbols

χ	rate of heat generation per unit volume (W m^{-3})
ϕ	circumferential angle variable
μ	dynamic viscosity (Pa s)
ν	kinematic viscosity (m^2 s^{-1})
ρ	density (kg m^{-3})
ω	disc speed (rad s^{-1})

Subscripts

c	cylindrical gap
d	disc
f	front face
r	rear face

inside of the pump casing, with a radial gap reduced to the practical minimum, to maximise shearing effect, of approximately 0.3 mm. Two interchangeable discs provided axial gaps of 0.3 mm and 1.0 mm, respectively. Liquid fed to the centre of the rotating disc is pumped radially outwards by centrifugal action. Heat is generated within the liquid, as it flows towards the outlet, as a result of internal friction or viscous dissipation. Liquid flows across the front face (nearer the liquid inlet) of the disc, through the disc/stator cylindrical gap and then into the casing cavity towards the outlet. Water and ethylene glycol were used as the working liquids.

Although this unit could by used to demonstrate that significant amounts of energy could be transferred by viscous dissipation, the unit was not suitable for a thorough study for the following reasons.

1. The installed disc was shrouded on only one face and across only 80% of the cylindrical area. The contributions of the unshrouded portion of the disc, and of the surrounding cavity, on heat generation and the flow field within the liquid, could not be determined.
2. The relatively small (130 mm) diameter of the discs limited the viscous dissipation energy generation rates to well below the 5.5 kW rating of the drive motor. A reduction in the disc/stator clearance below 0.3 mm to increase dissipation rates would have involved an unreasonable risk of contact between the disc and stator.
3. It was impossible to locate sensors through the casing and into the disc/stator gap, to measure temperatures and pressures.

2.2. Main study — purpose built machine

To overcome the above limitations a second rig was designed and built. A diagrammatic representation of the machine is shown in Fig. 2. The configuration of this machine was similar to that of the prototype. The main difference was that it had a larger disc (diameter 214 mm and width 39 mm) and a casing which enclosed front and rear faces, allowing greater dissipation energy levels to be demonstrated. It was also designed to allow provision of more comprehensive instrumentation to provide the data for a more accurate and thorough theoretical analysis of the machine.

Liquid was fed directly to the front face of the rotating disc; a part flowed through a central cavity (di-

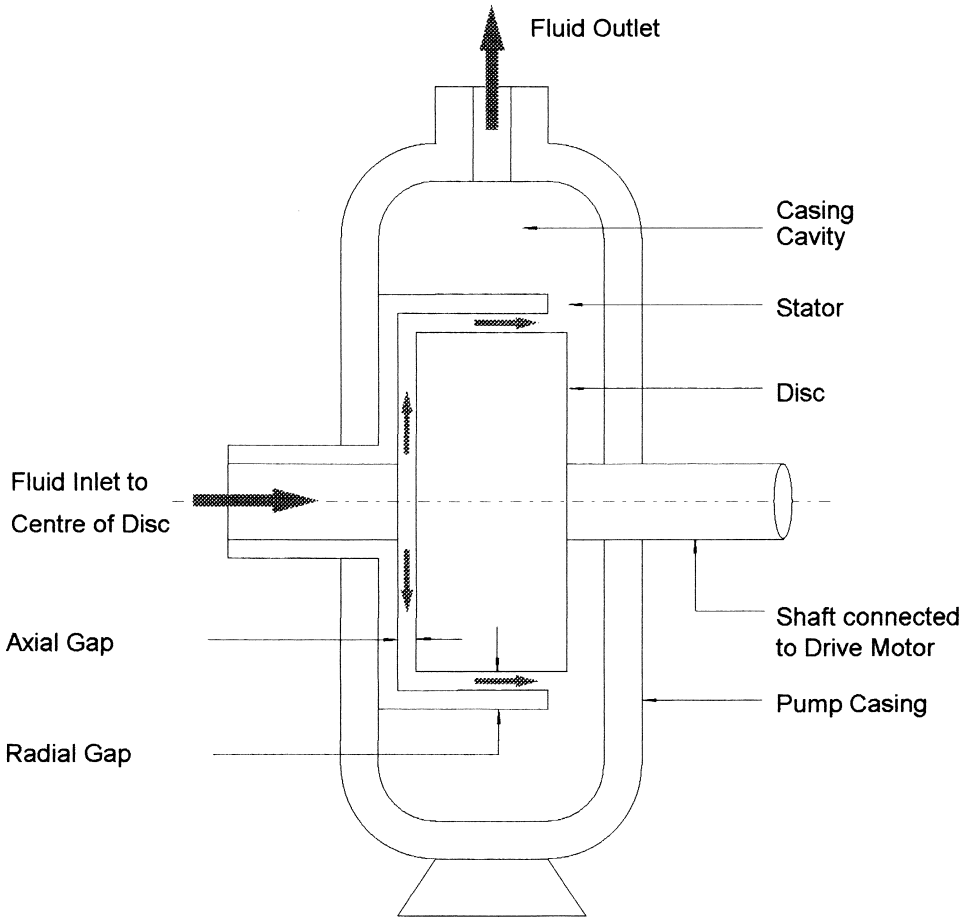

Fig. 1. Cross-section of the prototype viscous heating machine.

ameter 18 mm) in the disc and through a distributor to the rear face. The distributor consisted of six holes (diameter 3 mm), drilled radially at 60-degree angular increments around the drive shaft. Increased resistance to liquid flow to the rear face of the disc, due to the distributor, resulted in lower flows across the rear face. This effect is considered in the analysis of the results. The drainage channel in the casing was intended to help flow towards the outlet, and thus improve liquid distribution through the machine.

2.3. Gap measurement

The larger diameter disc allowed the radial and axial gap widths to be maintained at 1 mm, thus reducing the chance of contact between the disc and the casing. It was important to measure and confirm these gaps once the machine had been assembled, as any difference would have a significant effect on the accuracy of heat generation predictions. Prior to assembly the diameter of the disc and the internal diameter of the casing cavity were measured as 214 mm and 216 mm, respectively. After assembly, a feeler gauge was used to confirm the concentric location of the disc within the cavity, thus confirming the uniform 1 mm radial gap. Prior to assembly, the length of the disc, the depth of the casing cavity and the thickness of the cover plate were measured as 39 mm, 41 mm and 10 mm, respectively. After assembly, the distance between the outer surface of the cover plate and the front face of the disc was measured, using a depth gauge located through thermocouple tappings, as 11 mm. Thus confirmed the equality of the front and rear axial gap widths of 1 mm.

Mechanical considerations taken into account at the design stage included a check on vibration in the drive shaft, whirling or centrifugal effects on the disc, and relative thermal expansion between the disc and the casing. The entire machine was surrounded by a removable, insulated, aluminium box to limit heat losses. For more information the thesis of Ellwood [8], should be consulted.

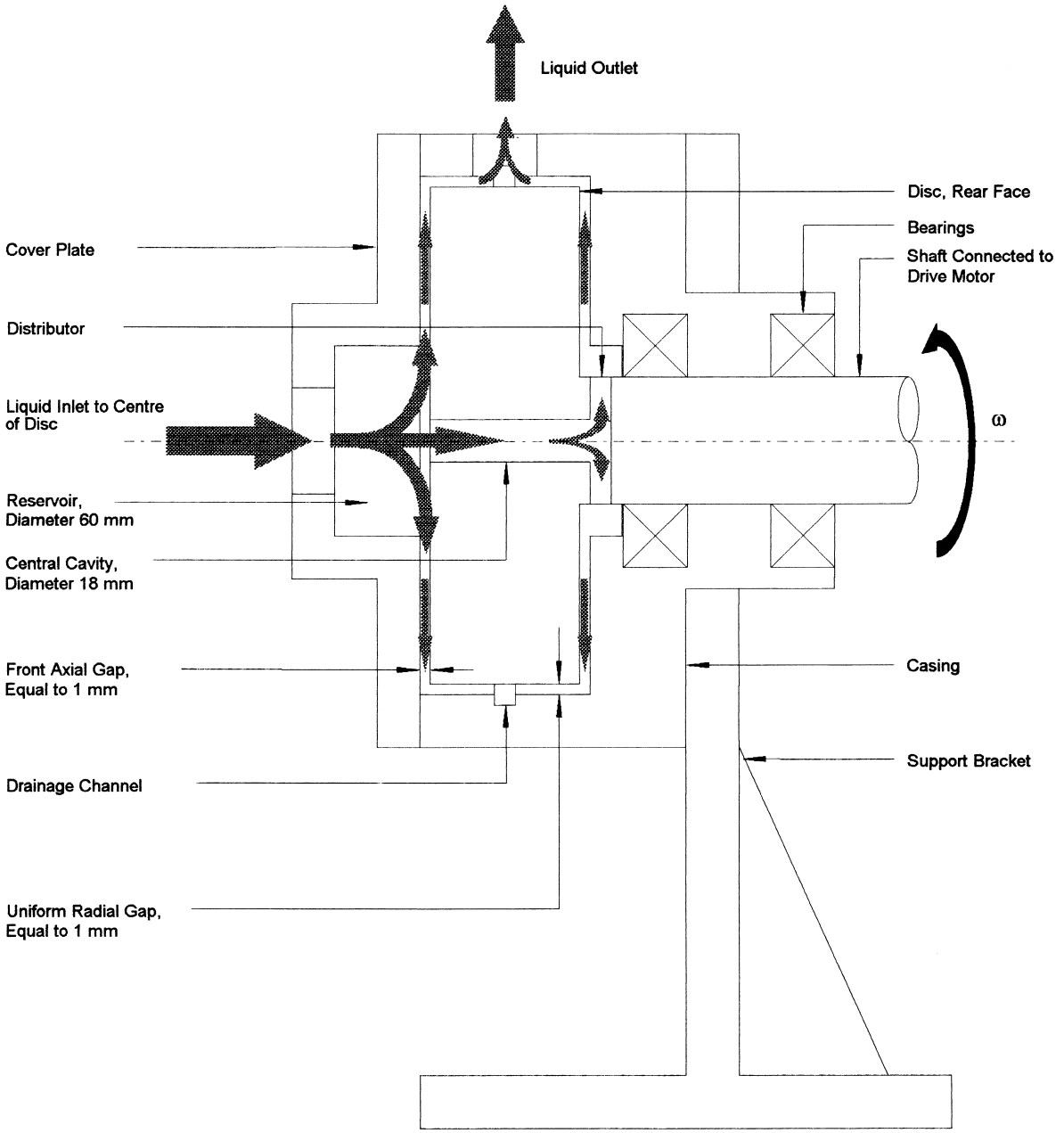

Fig. 2. Cross-section of the purpose built viscous heating machine.

2.4. Ancillary equipment

The viscous heating test rig system is illustrated in Fig. 3. The 5.5 kW electric drive motor from the modified Worthington–Simpson centrifugal motor/pump unit was also used to drive the purpose built machine. The motor was supplied with power from a Danfoss static frequency converter. This was used to provide a variable speed drive, and was adjusted to give control over the range 0–220 rad s^{-1}. The standard drive coupling between the motor and the machine was replaced with a proprietary IML Metastream torque measuring coupling, which permitted the measurement of the power input to the rotating disc unit.

The machine was connected into a supply and return pipework arrangement which incorporated supply and

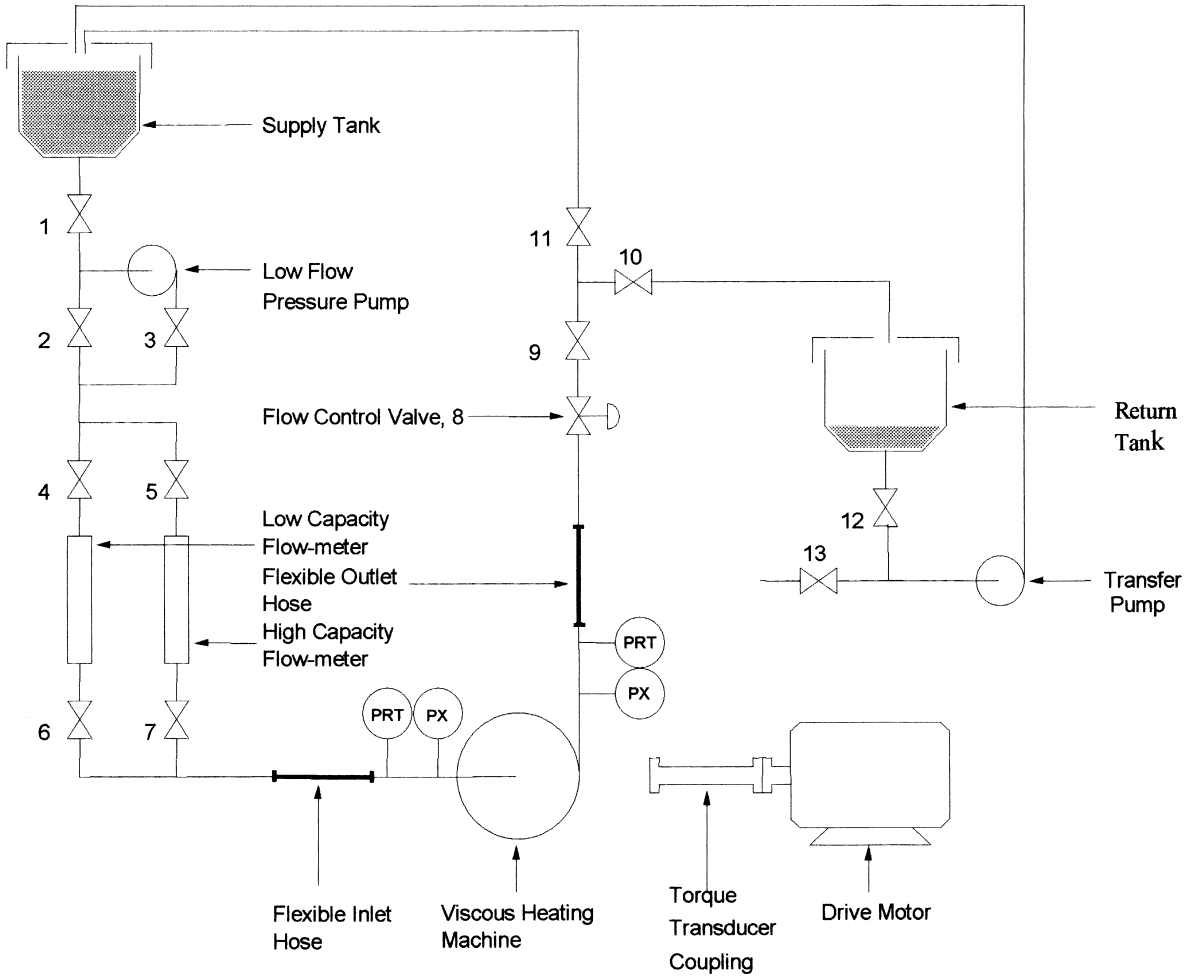

Fig. 3. Viscous dissipation rig.

return tanks (each with a capacity of 680 l), the appropriate flow control valves, variable orifice flow-meters and ancillary pump units.

Gravity induced flow, from the supply tank through the appropriate flow-meter and the viscous heating machine to the return tank, was the normal mode of operation. The original intention of the low flow pressure pump was for it to provide a boost to the flowrate of high viscosity liquids. However this pump proved unsuitable for this purpose. Thus the viscosity of the liquid used in the experimental programme was restricted to that which would flow through the rig under the influence of gravity. Flow through the viscous heating machine could be controlled, once a desired disc speed had been set, with the flow control valve located downstream of the machine. Liquid collected in the return tank could be pumped back to the supply tank using the transfer pump.

A Schlumberger ORION data-logger was used to monitor and record the data from the test rig instrumentation.

2.5. Working liquids

The two working liquids used in the viscous heating rig were (a) a proprietary automotive anti-freeze, ethylene glycol ($(CH_2OH)_2$) and (b) glycerol ($C_3H_5(OH)_3$—tradename Pricerine 9083). The glycerol was diluted with water, the proportion of volumes being approximately 80% glycerol and 20% water, in order to allow gravity flow to the rig. Using these two liquids enabled results to be generated over a range of viscosity. The methods of determination of viscosity, density and specific heat capacity characteristics are described below.

- Viscosity — a FS-722 cone and plate viscometer was used to determine the viscosities of the fluid used in

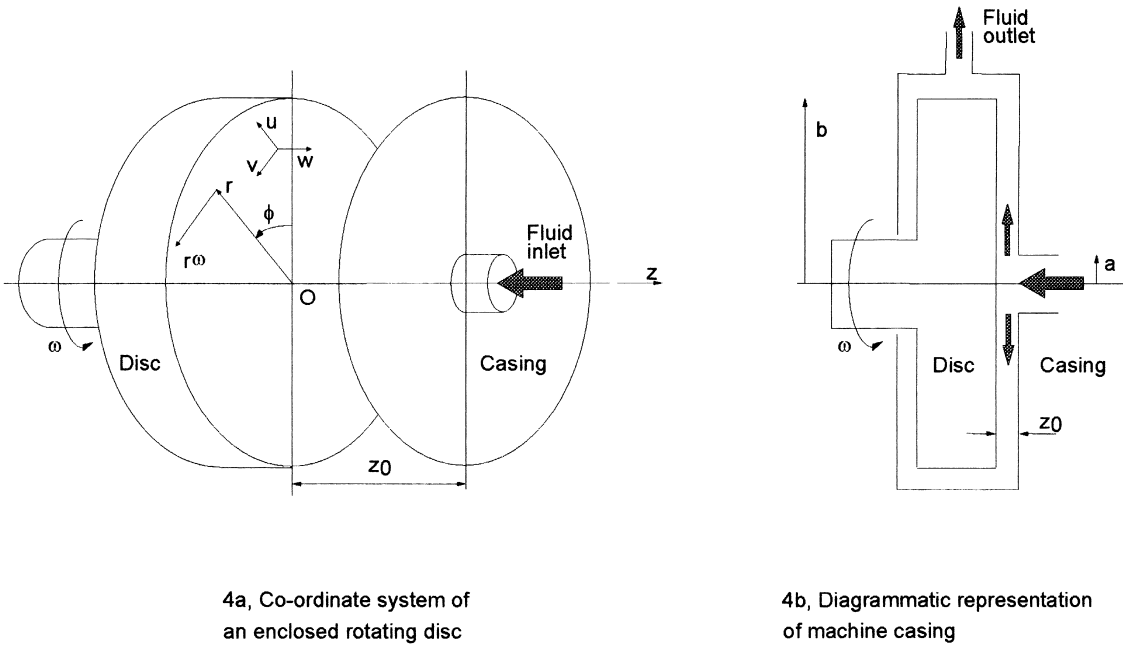

4a, Co-ordinate system of an enclosed rotating disc

4b, Diagrammatic representation of machine casing

Fig. 4. Co-ordinate system and diagrammatic representation of an enclosed rotating disc.

the study. The calibration of the viscometer was validated using a certified standard, a mineral oil, with a range of viscosities of between 0.0090 Pa s, at 300 K, and 0.00103 Pa s, at 293 K. The maximum error between reading and calibrated standard viscosity was 1%. Viscosities of ethylene glycol (in the range of 0.01–0.022 Pa s) were determined between 293 and 313 K, at the beginning and again at the end of the test series, a period spanning $3\frac{3}{4}$ months. The viscosities at the end were lower than those at the beginning, by about 5%, over most of the temperature range (300–313 K) and by as much as 10% at the lowest temperature (293 K). The higher initially calibrated values were used in analysing the results. Viscosities of dilute glycerol (in range of 0.03–0.065 Pa s) were also measured twice, with values before and after the tests (spanning 5 weeks) agreeing within 5%. The viscosity of ethylene glycol was found to vary from approximately 0.02 to 0.01 Pa s, over the temperature range 292–313 K, and the viscosity of dilute glycerol was found to vary from approximately 0.065–0.03 Pa s, over the temperature range 292–332 K.

- Densities were carefully measured, by weight and volume measurements, at room temperature, approximately 293 K, and assumed constant.
- Heat capacities were determined, over the range of temperatures used, with a Du Pont Thermal Analyst 2000 system. Measured values compared with published data to within the 2.5% accuracy claimed by the manufacturer.

2.6. Instrumentation

2.6.1. Temperature and pressure measurements

These were taken at six different positions. Platinum Resistance Thermometers (PRTs) and digital pressure transducers were located at the inlet and outlet reservoirs, which were immediately adjacent to the machine. These were used to determine the overall performance of the viscous heating machine. Enthalpy increases in the fluids were determined from the temperatures. The error in the enthalpy values were estimated by Ellwood [8] at ± 15 W. Thermocouples and digital pressure transducers also were located at 2 (front face) radial gap, and 2 cylindrical casing gap, positions and were used to measure local values within the disc/casing gaps. Triplicate readings, at 120^{o} intervals, were obtained in both gaps. No measurements were made on the rear face of the disc, because of the difficulty in locating instrumentation through the support bracket.

2.6.2. Torque measurement

An IML non-contacting system was used to measure dynamic torque, which was then used to calculate the shaft power input to the rotating disc. The two basic components in this system were the transducer and rotor electronics and the readout unit. A full bridge strain gauge assembly bonded to the inside wall of the coupling measured shear strain due to the applied torque. The output of the bridge was fed to the readout unit via the rotor electronics. An optical detector

was used to count shaft revolutions, which was converted to shaft speed by the data logger. The errors in shaft power input were estimated by Ellwood [8] at ± 18 W.

3. Theory

The following sections present the detail of the theory used to predict the performance of the purpose built viscous heating.

3.1. Regimes of flow in enclosed rotating disc systems

The experimental work carried out by Daily and Nece [9] resulted in the definition of four regimes which can be illustrated by plotting gap ratio, G, defined by

$$G = \frac{z_0}{b} \tag{1}$$

against Re_ϕ, defined by

$$Re_\phi = \frac{\rho\omega b^2}{\mu}. \tag{2}$$

For the value of G for the purpose-built machine of 0.0093, the transition between laminar and turbulent flow regimes is predicted to occur at a Re_ϕ of about 60,000. The Re_f value was below the transition value of 60,000 for all dilute glycerol results, increasing to a maximum value of 53,000 at the highest disc speed and lowest flow — corresponding to the highest temperature and lowest fluid viscosity. For the ethylene glycol results, all data at the highest disc speed of 125 rad s^{-1} were above the predicted transition Re value, and the data at the lower, 55 rad s^{-1}, disc speed straddled the transition value, with higher flow data below, and lower flow data above, the transition. The results explained below did not change significantly at the predicted transition.

3.2. Flow in enclosed rotating disc systems, with superposed laminar flow

3.2.1. Formulation of the problem

For the flow of fluid over an enclosed rotating disc, it is convenient to use a stationary frame of reference. The co-ordinate system used is shown in Fig. 4. The disc rotates about the z-axis with a constant angular velocity ω, in the direction of ϕ increasing. The direction of the z-axis points towards the casing, and the origin O is taken as the point where it intersects the disc. Thus the face of the disc lies in the plane $z = 0$ and the face of the casing lies in the plane $z = z_0$, where z_0 is the axial gap between the disc and the casing. The radius, or distance from the z-axis, is represented by the variable r, and the disc has an outer radius b.

The cylindrical polar co-ordinates (r, ϕ, z) are such that ϕ increases in the direction of a right handed screw relative to the positive direction of Oz. Referred to the fixed frame of reference, the velocity of a particle of fluid at any point (r, ϕ, z) is taken to be $\mathbf{v} = (u, v, w)$, its density, ρ, its temperature, T, and its pressure, p.

Fig. 4(b) shows a diagrammatic representation of the casing which encloses the disc. Fluid inlet is through the casing to the centre of the disc, the outlet is in the casing at the periphery. It is assumed that the inlet condition is simple radial source flow, starting from radius a, rather than the axial to radial flow that Fig. 4(b) suggests. It is also assumed that:

1. The flow is axisymmetric and steady, i.e. $\partial f/\partial\phi = \partial f/\partial t = 0$, for all dependent variables f.
2. The flow of fluid is laminar and as the gap ratio, G, is small, the boundary layers on the disc and casing are converged, i.e. Couette-type flow exists.
3. The fluid is incompressible and density, ρ, is constant.
4. The dynamic viscosity, μ, and the kinematic viscosity, ν, are constant.
5. The steady mass flowrate, m, can be considered to be small.
6. The flow is fully described by the continuity and Navier–Stokes equations.

3.3. Equations of motion

The equations of motion consist of the continuity and Navier–Stokes equations, in cylindrical co-ordinates, as follows:

Continuity equation

$$\frac{\partial u}{\partial r} + \frac{u}{r} + \frac{\partial w}{\partial z} = 0 \tag{3}$$

Navier–Stokes equations

$$u\frac{\partial u}{\partial r} + w\frac{\partial u}{\partial z} - \frac{v^2}{r} = -\frac{1}{\rho}\frac{\partial p}{\partial r} + \nu\left[\frac{\partial^2 u}{\partial r^2} + \frac{1}{r}\frac{\partial u}{\partial r} + \frac{\partial^2 u}{\partial z^2} - \frac{u}{r^2}\right] \tag{4}$$

$$u\frac{\partial v}{\partial r} + w\frac{\partial v}{\partial z} + \frac{uv}{r} = \nu\left[\frac{\partial^2 v}{\partial r^2} + \frac{1}{r}\frac{\partial v}{\partial r} + \frac{\partial^2 v}{\partial z^2} - \frac{v}{r^2}\right] \tag{5}$$

$$u\frac{\partial w}{\partial r}+w\frac{\partial w}{\partial z}=-\frac{1}{\rho}\frac{\partial p}{\partial z}+\nu\left[\frac{\partial^2 w}{\partial r^2}+\frac{1}{r}\frac{\partial w}{\partial r}+\frac{\partial^2 w}{\partial z^2}\right]. \quad (6)$$

3.3.1. Boundary conditions

The fundamental boundary condition is that, for any particle of fluid, a condition of no slip will exist at either the surface of the disc or the surface of the casing. Also, the radial, tangential and axial components of velocity, u, v, and w, are dependent upon the radius, r, and the axial dimension, z.

Thus the boundary conditions can be written:

$$u(r,0)=0;\quad u(r,z_0)=0$$

$$v(r,0)=r\omega;\quad v(r,z_0)=0$$

$$w(r,0)=0;\quad w(r,z_0)=0$$

$$2\pi\rho\int_0^{z_0} ru\,\mathrm{d}z=m \quad (7)$$

3.3.2. Soo simplified equations

Soo, in 1958 [2], further simplified the solution of the above equations by the introduction of the usual boundary layer approximations, which are:

1. The axial component of velocity w, is very much smaller in magnitude than either of the other two components.
2. The rate of change of any variable (other than the pressure) in the axial direction, i.e. the z direction, is much greater than its rate of change in a radial or tangential direction.
3. The pressure depends only on the radial distance from the axis of rotation.

The simplified equations then become

$$u\frac{\partial u}{\partial r}+w\frac{\partial u}{\partial z}-\frac{v^2}{r}=-\frac{1}{\rho}\frac{\partial p}{\partial r}+\nu\frac{\partial^2 u}{\partial z^2} \quad (8)$$

$$u\frac{\partial v}{\partial r}+w\frac{\partial v}{\partial z}+\frac{uv}{r}=\nu\frac{\partial^2 v}{\partial z^2} \quad (9)$$

$$\frac{\partial p}{\partial z}=0. \quad (10)$$

It should be noted that the boundary layer equations for the discs will not be valid in the neighbourhood of the shroud (the inner cylindrical surface of the casing), where the flow makes a sharp turn, nor near the axis of rotation, that is at the flow entrance to the disc gaps.

Soo solved the above for velocity and pressure profiles by assuming low flows and neglecting all inertia effects. The equations for the velocities in three dimensions were used to check the contributions of the velocity gradients other than the circumferential velocity gradient. In comparison to the latter, the remaining velocity gradients were confirmed to have a negligible contribution to viscous dissipation generation rates.

3.4. Viscous dissipation — disc gaps

To obtain the heat generated by viscous dissipation, only the term involving the axial variation of the circumferential velocity is required, that is

$$\chi=\mu\left(\frac{\mathrm{d}v}{\mathrm{d}y}\right)^2 \quad (11)$$

must be evaluated. The circumferential velocity varies linearly across the gap and is given by

$$v=r\omega(1-z/z_0). \quad (12)$$

Though this velocity can be obtained through the derivation of Soo, it can also be simply derived by assuming simple Couette flow between two radial disc surfaces, one of which is rotating at constant circumferential speed, $r\omega$. The energy generated per unit volume of fluid in the gap is therefore given by

$$\chi_{\mathrm{f}}=\mu\left(\frac{r\omega}{z_0}\right)^2. \quad (13)$$

This must be evaluated over the disc gaps, between $r=a$ and $r=b$, on either side of the rotating disc. The total heat generation rate, X_{f}, for each disc face is then given by

$$X_{\mathrm{f}}=\int_a^b\left[\mu\left(\frac{r\omega}{z_0}\right)^2 2\pi r z_0\right]\mathrm{d}r \quad (14)$$

or

$$X_{\mathrm{f}}=\left[\frac{\pi r^4\mu\omega^2}{2z_0}\right]_a^b \quad (15)$$

or

$$X_{\mathrm{f}}=\frac{\pi b^4\mu\omega^2}{2z_0}-\frac{\pi a^4\mu\omega^2}{2z_0}. \quad (16)$$

3.5. Viscous dissipation — disc cylindrical gap

The same Couette-flow model can also be applied to the cylindrical region of the disc, rotating in close proximity to the stationary casing. The tangential velocity of the cylindrical face of the disc, at outer radius

b, rotates at a constant angular velocity, bw. Given that there is a radial gap, y_0, between the disc and the casing, the rate of heat generation per unit volume is given by

$$\chi_c = \mu\left(\frac{b\omega}{y_0}\right)^2. \tag{17}$$

As the total volume within a particular half of the cylindrical region, of length $l/2$, is given by $2\pi b y_0 l/2$, the total heat generated within each half of the cylindrical gap region is given by

$$X_c = \mu\left(\frac{b\omega}{y_0}\right)^2 2\pi b y_0 l \quad \text{or} \quad \therefore X_c = \frac{2\pi\mu b^3\omega^2 l}{y_0}. \tag{18}$$

3.6. Total viscous heat generation

Combining the expression for total heat generation for flow across the two disc faces, given in Eq. (16), with the expression for total heat generation across the disc cylindrical gap region, given in Eq. (18), gives the total heat generation rate as:

$$X_d = \frac{\pi b^4\mu\omega^2}{2z_0} - \frac{\pi a^4\mu\omega^2}{2z_0} + \frac{2\pi\mu b^3\omega^2 l}{y_0}. \tag{19}$$

This was the equation used to predict the total heat generation by viscous dissipation for the viscous heating machine.

3.7. Radial pressure variation

The average radial pressure change across the face of the disc was given by Soo [2], as

$$\begin{aligned} p_b - p_a \cong (0.5\rho b^2\omega^2)\Bigg[&\left(\frac{-3}{\pi}\right)\left(\frac{m}{\rho z_0\omega b^2}\right) \\ &\times\left(\frac{1-0.078968Re_z^2}{Re_z}\right)\ln\left(\frac{b}{a}\right) \\ &+\left(\frac{3}{10\pi^2}\right)\left(\frac{m}{\rho z_0\omega b^2}\right)^2\left(\frac{b^2}{a^2}-1\right) \\ &+\left(\frac{2}{5}\right)(1+0.001095Re_z^2)\left(1-\frac{a^2}{b^2}\right)\Bigg]. \end{aligned} \tag{20}$$

The first term on the RHS of Eq. (20) accounts for the pressure change due to frictional loss across the face of the disc. The second term accounts for the pressure change due to diffusion as the fluid expands radially outwards towards the periphery. The third term represents the pressure change due to the centrifugal effect.

3.8. Energy measurements

An energy balance on a given mass of fluid gives

$$\Delta U_1 + \Delta\left(\frac{p}{\rho}\right) + \Delta\left(\frac{v^2}{2}\right) + g(\Delta z) = Q - W_s. \tag{21}$$

The following assumptions were made:

1. Liquid density, ρ, remained constant over the range of operating temperatures.
2. Mean velocity, v, remained unchanged across the machine (as the reservoirs at positions 1 and 6, the inlet and outlet of the machine, were of the same diameter), so $\Delta(v^2/2)=0$.
3. The difference in height between the reservoirs at positions 1 and 6, the inlet and outlet of the machine was negligible (position 1 was 0.3 m above position 6), so $g\Delta z \approx 0$.
4. The purpose built viscous heating machine was well insulated from the surroundings by an insulated aluminium box, therefore the heat loss to atmosphere, Q, was assumed to be negligible (the difference between the sum of the values on either side of the equation may be an indication of the magnitude of Q).

Thus Eq. (21) becomes:

$$\Delta U + \frac{\Delta p}{\rho} = \Delta H = -W_s. \tag{22}$$

This means that the power put into the shaft driving the rotating disc is expended either into heating the fluid or into raising its pressure. If there are no heat losses the measured quantities on either side of the equation should balance. Changes in enthalpy, ΔH, are assumed to be due only to changes in temperature, and heat capacities are constant over the range of temperature encountered, so

$$\Delta H = C_p\Delta t. \tag{23}$$

With the pump running and significant dissipation energy being generated, the internal energy term far exceeds the pressure term.

With the pump down and the disc stationary, for a given flow of fluid through the pump, there is a significant friction loss, which results in a very small increase in internal energy. To obtain the net contribution of the shaft power to pressure energy, the difference in overall pressure change must be determined between the pump running and the pump stationary.

The net pressure change, across the face of the disc, is predicted by Eq. (20). The additional pressure change, due to frictional losses downstream of the disc face, were estimated from measured pressure changes with the disc stationary. These must be added to the

Soo-predicted values to compare the total with the total measured pressure drop with the disc rotating. The frictional losses beyond the disc face are assumed to be unaffected by the rotation of the disc. These were estimated by subtracting the Soo-predicted pressure change for a stationary disc, from the measured overall pressure change with the disc stationary. Since the former were very small, the latter were essentially the pressure change due to frictional losses beyond the disc face.

3.9. Flow to the front and rear faces of an enclosed rotating disc

The difficulty in analysing the above changes was that only the total flow to the front and rear face of the disc were measured. On entering the machine, the flows divided, as shown in Fig. 2, to the front and rear gaps. Thus flow distribution to the two gaps occurred on the basis of the pressure drops present in each of the paths, with considerably less flow to the rear gap, due to increased resistance due to the distributor. This was confirmed by the higher temperature changes at the rear face. The split in flows was determined by the difference in the temperature change resulting across the two gaps, assuming that the dissipation energy generated in each gap was the same.

The measured overall mass flowrate, m, at the machine inlet splits into a flow, m_f, across the front face of the disc, and a flow, m_r, across the rear face of the disc. Assuming heat generation rates are the same for the front and rear faces of the disc, these flowrates can be determined from the respective changes in enthalpy, using

$$\Delta H_f m_f = \Delta H_r m_r \tag{24}$$

where ΔH_f is the change in fluid enthalpy across the front face of disc (J kg^{-1}) and ΔH_r is the change in fluid enthalpy across the rear face of disc (J kg^{-1}).

The enthalpy changes can be determined from measured temperatures at the exit of each gap. If the heat capacities are assumed constant over the relatively small temperature change, the individual flows may be determined from the measured temperatures as follows:

$$\therefore m_f = \frac{(T_5 - T_1)m}{T_4 + T_5 - 2T_1} \tag{25}$$

and

$$\therefore m_r = \frac{(T_4 - T_1)m}{T_4 + T_5 - 2T_1}. \tag{26}$$

Table 1
Typical data produced with prototype device

Fluid	Viscosity (Pa s)	Flow (m^3 min^{-1} $\times 10^3$)	Disc speed (rad s^{-1})	Temperature increase (K)	Energy gain by fluid (W)	Energy input by motor (W)	Energy predicted by dissipation (W)
Water	0.001	1.0	314	3.3	231	34	27
Ethylene glycol	0.008	0.5	307	16.4	369	383	226

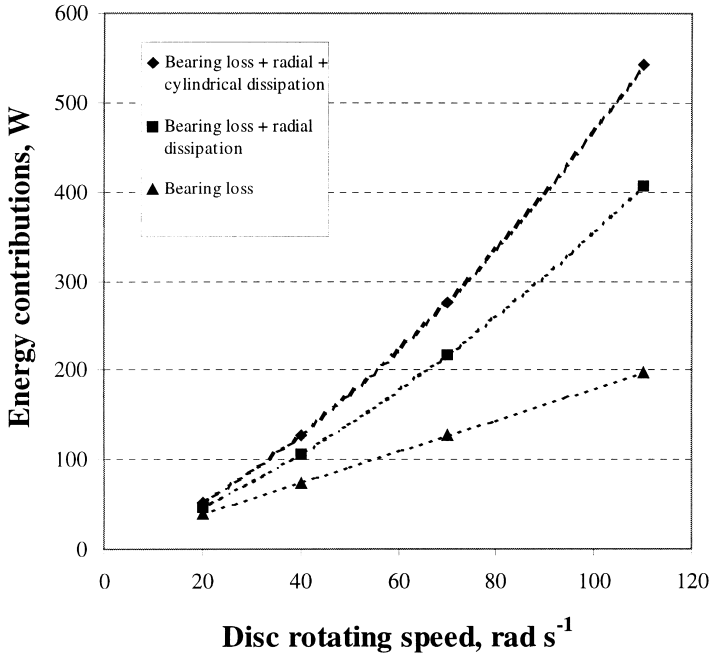

Fig. 5. Comparison of predicted dissipation rates and bearing losses.

4. Results

4.1. Prototype device

This device successfully demonstrated that viscous fluids could be heated through viscous dissipation in this kind of device, and encouraged the construction of the purpose-built device. Tests of the instrumentation and control apparatus were successfully demonstrated. The viscosity of ethylene glycol was found to vary from approximately 0.02 to 0.01 Pa s, over the temperature range 292–313 K, providing a 10-fold increase in viscosity over that of water. Typical of the data produced with this device were those in Table 1.

Water results were inaccurate because the torque levels were too low for the torque-meter, and the temperature increases were very small. Generated enthalpy increases in the ethylene glycol more closely matched the power input obtained from the torque measurements. However, for both systems, predicted viscous dissipation effects were much lower than measured effects. The inability to take sufficient measurements to explain this led to the construction of the new device.

4.2. Purpose-built device

Ethylene glycol and water-diluted (20% by volume) glycerol were passed through this heating device over a range of conditions, summarised by the following values:

- flows varied between 2 and 50 ml s^{-1} or 0.0022 and 0.08 kg s^{-1}
- viscosities varied between 0.01 and 0.065 Pa s
- rotating disc speeds varied from 0 to 125 rad s^{-1}.

Early results indicated that energy values measured by the fluid temperature increases and by torque measurements, just as in the prototype tested earlier, far exceeded those predicted for viscous dissipation heating. This is because there were two mechanisms by which fluids passing through the machine were being heated. These were as follows:

1. Viscous dissipation heating due to the high velocity gradients in the narrow disc and cylindrical gaps.
2. Conduction from the heated casing, which resulted from the heat generated in the shaft bearings.

When the contribution of the second was accounted for by measuring the power required to drive the disc with the device empty of fluid, the contributions of both the above accounted accurately for the total energy transferred to the fluid. At low disc speeds in fact, the heat generated by the bearings exceeded that from viscous dissipation, but at higher disc speeds the predicted viscous dissipation rates were higher than the bearing-generated losses. This is illustrated for one flow of diluted glycerol in Fig. 5. Construction of this type of heating device would obviously have to be more carefully carried out so that friction losses in the bearings would be greatly reduced.

With viscous fluid flowing through the device at

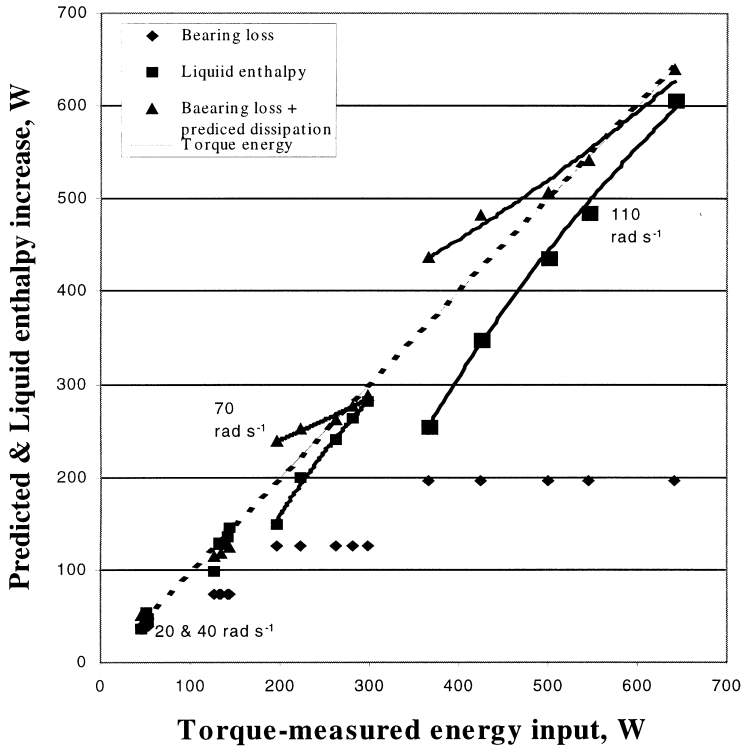

Fig. 6. Comparison with energy calculated from torque measurements of (i) total energy transfer by liquid enthalpy increase, and of (ii) bearing loss + predicted viscous dissipation energy.

various flows, comparisons were made between the following total energy transferred.

1. The sums of the energy generated by the two effects above.
2. The total energy supplied to the machine, measured with the torque-meter.
3. The total energy transmitted to the liquid (measured by the enthalpy increase) passing through the machine. There was proportionately a very small increase in pressure energy.

The results obtained for diluted glycerol will be used to illustrate the influences found. The ethylene glycol results were very similar.

As indicated in Fig. 6 there was close agreement between the above three values, especially so at the higher flow rates through the machine, where the lower temperatures generated resulted in lower heat losses to the surroundings. At the higher flows the differences between the total energy transfers (1) by the total of bearing loss (also plotted) and viscous dissipation, (2) by torque measurement, and (3) by measured liquid enthalpy increase, were within 20 W in most case, consistent with estimated experimental errors. As indicated in the data below, at the lowest flows, and the highest disc speed — of 110 rad s^{-1}, predicted energy additions due to dissipation and bearing friction were higher, by as much as 70 W, than measured shaft input power, and measured enthalpy increases were as much as 110 W, or 30%, below the measured shaft input power. The poorer agreement in the latter case was probably due to higher heat losses due to the higher temperatures generated at the lower flows. As the flows decrease, and fluid temperatures

Table 2
Summarised deviations from torque-measured energy levels (disc speed — 110 rad s^{-1})

Fluid flow, kg s^{-1}	0.0024	0.0060	0.0120	0.0241	0.0605
Fluid temperature rise, °C	35	20	13	7.5	3.8
'Heat loss', W	109	76	64	58	34
Predicted − measured, W	71	58	7	−2	−1

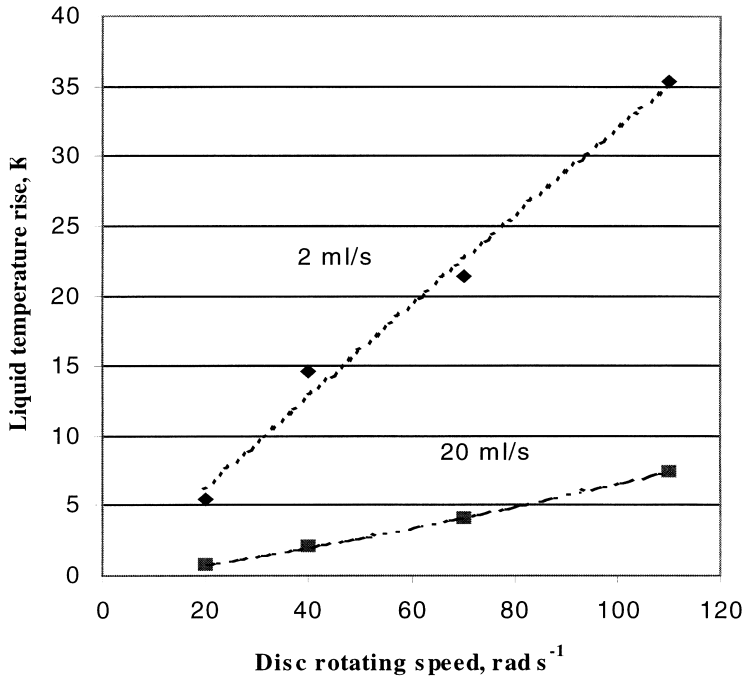

Fig. 7. Measured liquid temperature increases.

generated increase, contributions of heat losses become more prominent. If the differences between the torque-measured energy input and liquid enthalpy increase are assumed to be due to heat loss, the relationship between heat loss and generated fluid temperature is very obvious, as indicated in Table 2.

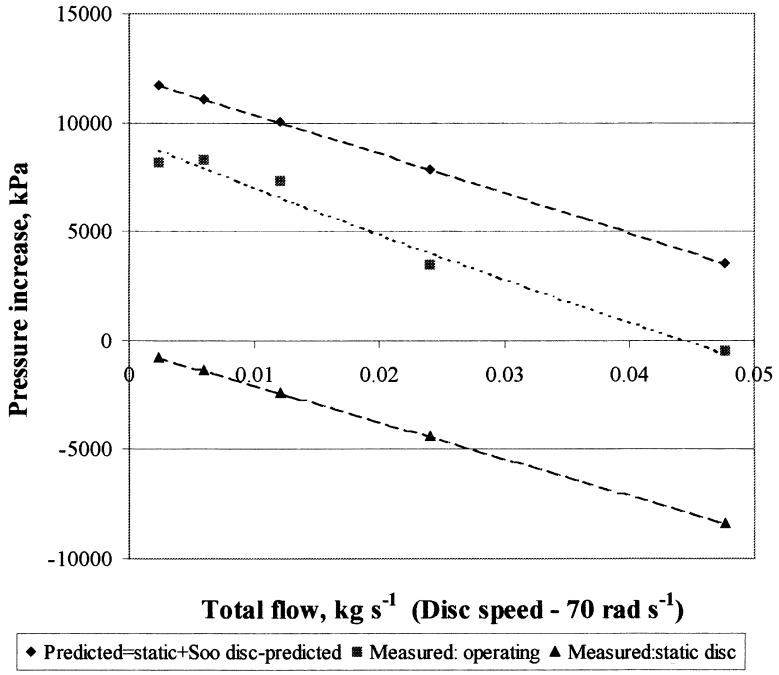

Fig. 8. Overall pressure change across the rig: comparison of (i) measured and (ii) predicted from static pressure drop plus Soo-predicted, disc-generated, pressure increase across the disc (constant speed of 70 rad s^{-1}).

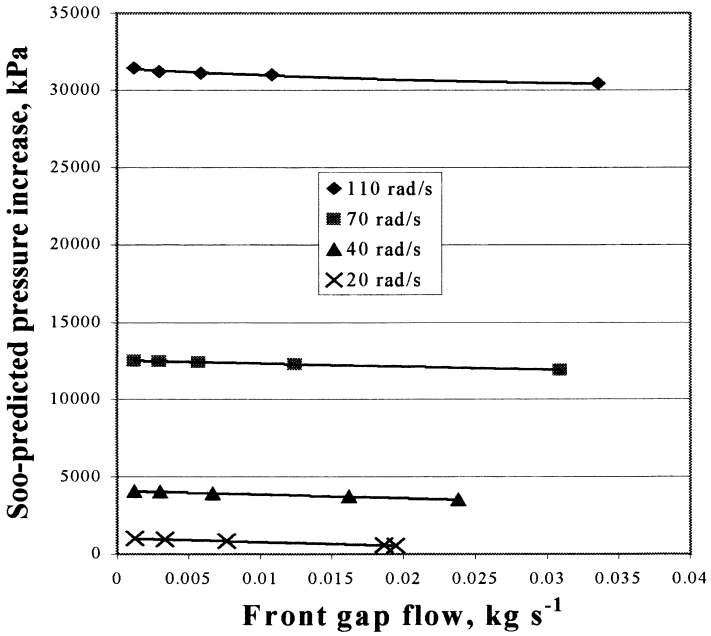

Fig. 9. Soo-predicted, disc-generated, pressure increase across the disc; dependence on disc rotating speed and actual flow through the front gap.

As the predicted values included dissipation energy generated and bearing losses, the deviation from measured value at low flows could be caused by errors in either. It is assumed that measured bearing losses with the machine empty of liquid applied also to operation with liquid in the machine. Although the largest deviations do occur under conditions where the Re_ϕ approached the transition between laminar and turbulent flow (see Theory), this is not the cause, as predicted turbulent conditions for the ethylene glycol runs at high disc speeds did not give the same deviations.

It should be noted that energy generation rates increase with flows at a given disc speed due to the influence of viscosity increases on viscous dissipation rates. Viscosities increase with increases in flow as a result of lower temperature increases.

In all cases, over 99.5% of the energy transferred to the liquid contributed towards increasing its temperature, or internal energy, and less than 0.5% contributed towards increasing pressure head. The maximum measured heating power was 0.6 kW. This was achieved at a disc speed of 110 rad s^{-1} and a dilute glycerol flowrate of 0.0605 kg s^{-1}. Temperature increases obtained in the machine are plotted in Fig. 7. They increase with disc speed and decrease as flows increase. The maximum measured overall temperature increases recorded for ethylene glycol was 41.6 K at a disc speed of 125 rad s^{-1} and a mass flowrate of 0.0024 kg s^{-1}, and for dilute glycerol was 35.4 K, at 110 rad s^{-1} and 0.0024 kg s^{-1}.

Results showed that average temperature increases recorded for flows across the rear of the disc were consistently higher, by up to a factor of 2, than those recorded for flow across the front of the disc. This confirmed that there was reduced flow across the rear face of the disc due to the restriction of the rear face distributor. This is discussed further below.

4.3. Pumping

Although the contribution of the power input to the liquid pressure head was relatively very low, significant pressure increases were generated. At higher disc speeds, of 70 rad s^{-1} illustrated in Fig. 8, positive overall pressure head was added over almost the entire range of flows. The viscous heating machine was acting as a pump in addition to its main function as a heating device.

The pressure change due to the centrifugal effect across the faces of the disc was predicted to be dominant at all disc speeds, and this dominance increased significantly with increasing disc speed. The total pressure change across the disc radial surface was small in comparison with that downstream of the disc, which included the disc cylindrical region, the machine exit, and the rear face distributor.

Only the pressure increase through the disc radial

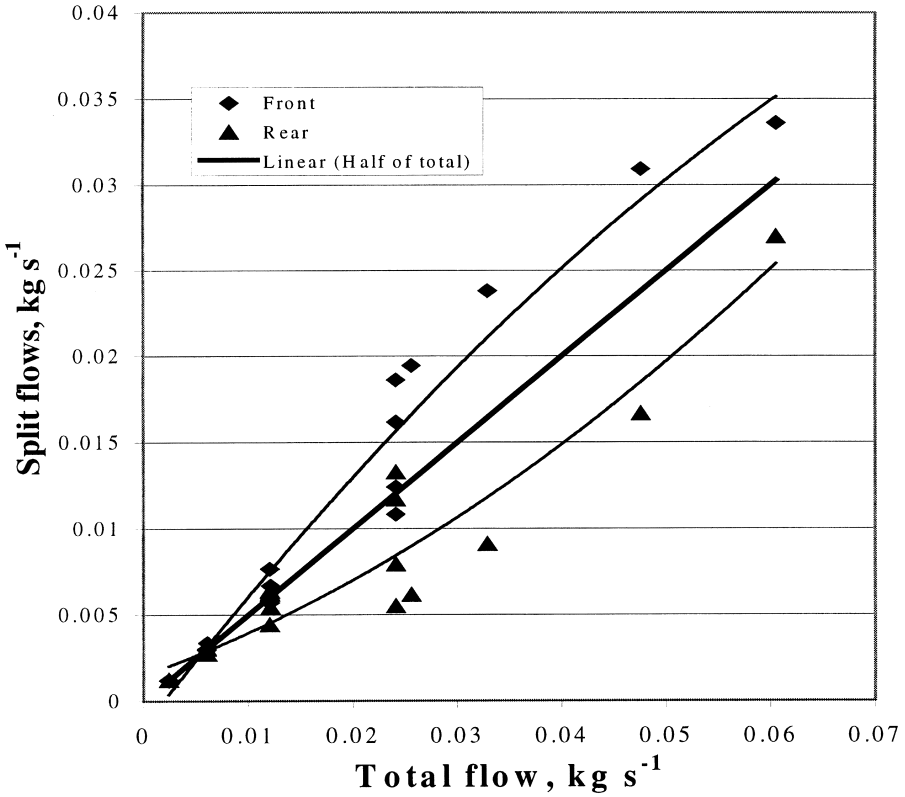

Fig. 10. Difference in flow between front and back of rotating disc.

gap could be predicted from Soo's resulting equation. These are plotted in Fig. 9. These could not be measured to obtain a direct comparison with predicted results. Instead, the predicted values were added to the estimated pressure change downstream of the radial gap. The pressure drop downstream was determined by subtracting the predicted disc face pressure drop from the overall pressure drop, for a stationary disc. The measured total pressure drops with the disc running were then compared with the sum of the downstream pressure drops for a stationary disc and the pressure drop across the disc predicted by Soo for a rotating disc. The predicted influence of the rotating disc was greater than the measured influence, as indicated by the lower measured pressure increases in Fig. 8.

Before the Soo [2] predictions could be made the individual flows to either side of the disc had to be determined, using the differences in the temperature increases, as indicated earlier. The resulting calculated split in the total flows is illustrated in Fig. 10. This indicates that at low flows there is an almost even split between the flows to the front and back gaps, but as the flows increase, the pressure drop to the rear gap increases more rapidly and the flow increases are smaller than to the front gap.

5. Conclusions

The use of a high speed rotating disc, and a narrow gap, to heat and pump viscous fluids, has been demonstrated. Theoretical predictions of viscous dissipation rates were near those obtained experimentally. Further work is now required to show the commercial viability of such means of heating.

Acknowledgements

The authors would like gratefully to acknowledge the financial assistance obtained under the EA Technology/UMIST Postgraduate Training Partnership (PTP), which provided financial assistance from the Engineering and Physical Sciences Research Council, the Department of Trade and Industry and EA Technology.

References

[1] W. Froude, A new dynamometer for measuring the power delivered to the screws of large ships, Proceedings of Institution of Mechanical Engineers 72 (1877) 237–275.

[2] S.L. Soo, Laminar flow over an enclosed rotating disk, Trans. ASME 80 (1958) 287–296.
[3] L.A. Dorfman, Hydrodynamic Resistance and the Heat Loss of Rotating Solids, 1, Oliver and Boyd, Edinburgh, 1963.
[4] J.M. Owen, R.H. Rogers, Flow and Heat Transfer in Rotating-Disc Systems, Research Studies Press Ltd, Taunton, 1989.
[5] E.R.G. Eckert, R.M. Drake, Heat and Mass Transfer, McGraw-Hill, London, 1959.
[6] R. Wander, R. Angue, Approvisionement-transport aerien-distribution. Apparatus for sterilisation or pasteurisation, UK Patent 1370033, vol. 39448/72, 1975.
[7] A. Schmitt, A.G. Wuwa, A Process and apparatus for sterilising fluids, UK patent 2095971 B, vol. 8208103, 1984.
[8] C.M. Ellwood, The heating, by viscous dissipation, of liquids flowing across an enclosed rotating disc, PhD Thesis, UMIST, 1996.
[9] J.W. Daily, R.E. Nece, Chamber dimension effects on induced flow and frictional resistance of enclosed rotating discs, Transactions of the ASME — Journal of Basic Engineering 82 (1960) 217–232.